# The behaviour and detection of partial thermal thermoremanent magnetisation (pTRM) tails in Thellier palaeointensity experiments

A. J. Biggin, Mireille M. Perrin

*Earth Planets Space*, **59**, 717–725, 2007

# The behaviour and detection of partial thermoremanent magnetisation (PTRM) tails in Thellier palaeointensity experiments

Andrew J. Biggin[1,2] and Mireille Perrin[1]

[1]*Laboratoire Tectonophysique, ISTEEM, Université Montpellier II, CC049, Montpellier, 34090, France*
[2]*Palaeomagnetic Laboratory Fort Hoofddijk, Universiteit Utrecht, Utrecht 3584 CD, Netherlands*

(Received September 27, 2006; Revised February 15, 2007; Accepted March 3, 2007; Online published July 20, 2007)

We analyse the results of Thellier palaeointensity experiments modified so that the measured magnetisation at any stage may be decomposed into components of natural remanent magnetisation (NRM) and laboratory thermal remanent magnetisation (TRM). We demonstrate that the very long high temperature tails of pTRM acquired by multidomain (MD) grains may be detected in Thellier experiments without recourse to explicit pTRM tail check measurements. This can save time in the experimental process and provides a more sensitive indication of how MD behaviour may affect that particular experiment than either pTRM tail checks or the observation of zigzagging in an IZZI experiment. We observe that the action of imparting a pTRM tail also involves some removal of NRM. However, the pTRM tails are not the analogues of classical overprints as may be intuitively expected but instead appear to favour remagnetisation over demagnetisation. This and other observed behaviour is not consistent with any phenomenological model of MD TRM but is consistent with predictions made by kinematic theory.

**Key words:** Paleointensity, thermoremanent magnetisation, pTRM tails, multidomain grains.

## 1. Introduction

Single domain grains do not uniquely carry the permanent magnetisation of the overwhelming majority of igneous rocks. Rather, multidomain and 'pseudo-single domain' ferromagnetic grains (to be collectively referred to as 'multidomain' from hereon) are also present and may dominate the remanent magnetisation in a large number of cases. Such grains do not behave in as simple a manner as single domain (SD) grains and violate Thellier's (1938) laws of thermoremanent magnetisation to a greater or lesser degree. This violation is most evident in disparities between the blocking ($T_b$) and unblocking ($T_{ub}$) temperatures of partial TRMs leading to high ($T_{ub} > T_b$) and low ($T_{ub} < T_b$)-temperature *tails* of pTRM.

Since their discovery by Shashkanov and Metallova (1972) and Bol'shakov and Shcherbakova (1979), these tails have been subject to much scrutiny (e.g. Dunlop and Özdemir, 2001; Shcherbakov *et al*., 2001b). Most recently, Biggin and Poidras (2006) demonstrated that it is more intuitive in most cases to regard low-temperature tails of pTRMs as high temperature tails of demagnetisation treatments.

The differences between SD and MD TRM have important implications for practical palaeomagnetic studies. One of these, discovered by Levi (1977), is that Thellier palaeointensity experiments performed on samples dominated by MD grains produce Arai plots that, unlike like those produced by SD samples, are not linear. Because of this Arai-plot curvature, strong MD-type TRM behaviour can cause the palaeointensity to be determined wrongly. It is vital therefore that such behaviour can be detected in samples so that their determinations can be rejected.

The most common method of determining the degree to which a sample may exhibit MD behaviour in a palaeointensity experiment is to measure its hysteresis properties and, based on these, to categorise its average properties as SD, PSD (pseudo-single domain), or MD. Very few igneous rock samples have SD-like bulk hysteresis properties. However, Biggin and Thomas (2003) demonstrated that even samples defined as PSD in these terms may produce significantly inaccurate palaeointensity determinations.

Ferromagnetic grain assemblages in rocks can be extremely complex so that the bulk hysteresis properties of a sample and its behaviour in palaeomagnetic experiments may be determined by different sets of magnetic grains. Consequently, methods which detect MD TRM behaviour directly are better for screening samples for reliability as palaeointensity recorders. Various experiments designed to characterise samples through direct measurements of their pTRM tails have been proposed (Bol'shakov and Shcherbakova, 1979; Goguitchaichvili *et al*., 2001; Perrin, 1988; Shcherbakov *et al*., 2001a). However, these have not been widely used in palaeointensity studies on account of them being time consuming, causing samples to alter prior to characterisation, or requiring equipment which is not in place at most laboratories.

Currently, the most popular means of detecting MD behaviour in samples subject to palaeointensity experiments is to use *pTRM tail checks* in the experiments themselves (Riisager and Riisager, 2001). These are effective and efficient

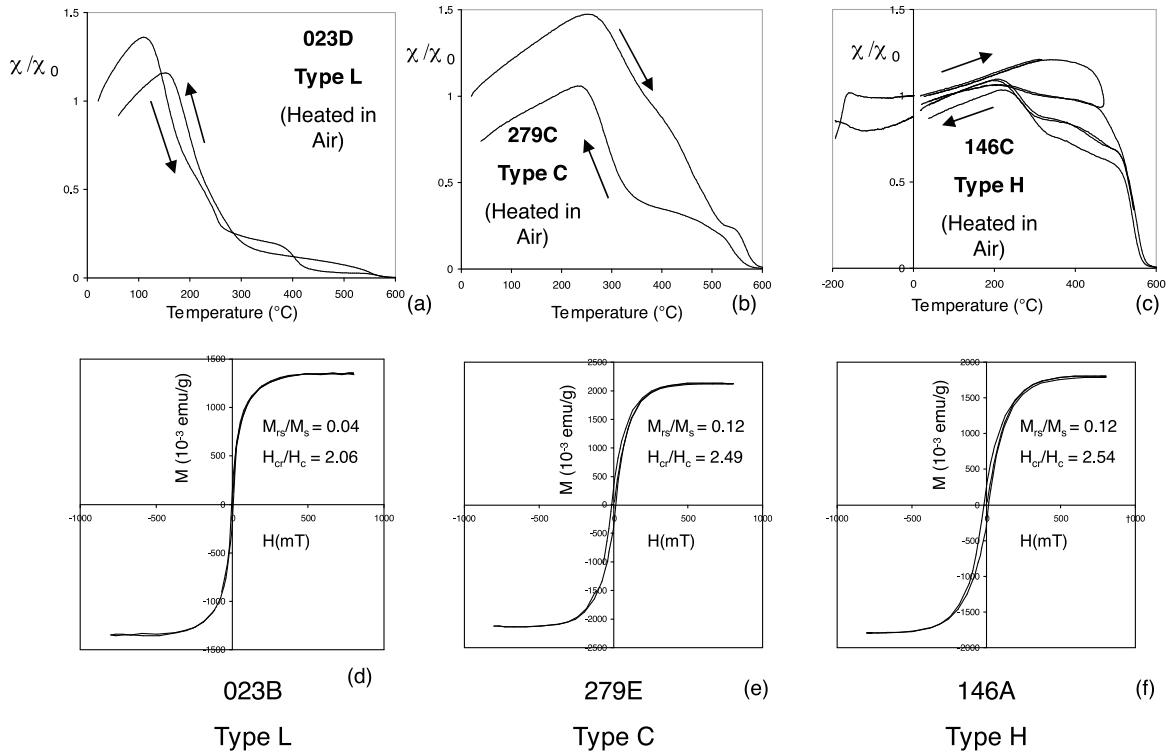


Fig. 1. Temperature dependence of low-field susceptibility and hysteresis loops for specimens taken from the same core samples as those used for palaeointensity analysis in this study.

means of assessing the degree of MD behaviour in a sample providing that the vector of the magnetic field applied in the experiment is not similar to the vector of the palaeofield (Yu and Dunlop, 2003). More recently, Tauxe and Staudigel (2004) outlined the IZZI variant of the Thellier method of determination which can allow MD behaviour to be detected without the necessity for specific pTRM tail checks.

A very detailed rock magnetic and palaeointensity study was recently performed on samples from the Mount Etna volcano. This article will focus on the results of one of the palaeointensity experiments undertaken as part of this study and use them to improve our understanding of MD TRM behaviour in Thellier experiments. Specifically, previously unknown attributes of pTRM tails and an improved means of detecting them will be outlined.

## 2. Samples and Experimental Methodology

The samples used in this study were taken from various basalt flows which were emplaced on the slopes of Mt Etna in the 20th Century. Their rock magnetic properties will be described in detail elsewhere (Biggin *et al*., 2007a) so only brief discussion will be given here.

Measurements of the variation of low-field susceptibility with temperature were used to produce $\chi(T)$ curves from a total of 81 specimens (e.g. Fig. 1(a)–(c)). These showed that four distinct ferromagnetic phases were present, often in combination, within the samples. The Curie temperatures of these four phases were observed to vary between 150 and 580°C which, together with microscopic analyses, revealed that they were titanomagnetites oxidised to varying degrees (one close to primary TM60, another close to pure magnetite, and two intermediate phases). Samples were characterised according to the relative dominance of the phases in the $\chi(T)$ curves into L (low), C (combination), and H (High) type. Examples of these three categories of curves are provided in Fig. 1. Cyclic $\chi(T)$ measurements suggested that thermochemical alteration of all samples was negligible below 350°C.

The hysteresis properties of the samples vary between multidomain and coarse pseudo-single domain (Fig. 1(d)–(f)). Measurements of the laboratory Königsberger ratio ($Q_L$) and the viscosity index (VI), as described by e.g. Prévot *et al*. (1981), were made for specimens from all core samples. These, together with other rock magnetic parameters measured for the samples used in this study are also given in Table 1. Interestingly, while the L type samples were the most 'MD-like' in terms of their hysteresis properties and measured values of $Q_L$ and VI, the same was not true of their behaviour in the palaeointensity experiments as will be described and explained below.

Palaeointensity experiments were performed using the laboratory-built oven at Université Montpellier II which has a residual field of less than 10nT and maintains a vacuum during heating and cooling better than $10^{-5}$ Torr ($10^{-3}$ Pa). Measurements were made using a JR5 spinner or 2G cryogenic magnetometer.

The basic palaeointensity protocol we used was identical to Thellier and Thellier's (1959) method as adapted by Coe (1967) and featuring pTRM and pTRM tail checks (Riisager and Riisager, 2001). This consisted of the following thermomagnetic treatments made at each temperature $T_i$:

1. The *demagnetisation* treatment (heating and cooling between room temperature, ($T_r$) and $T_i$ in zero field).

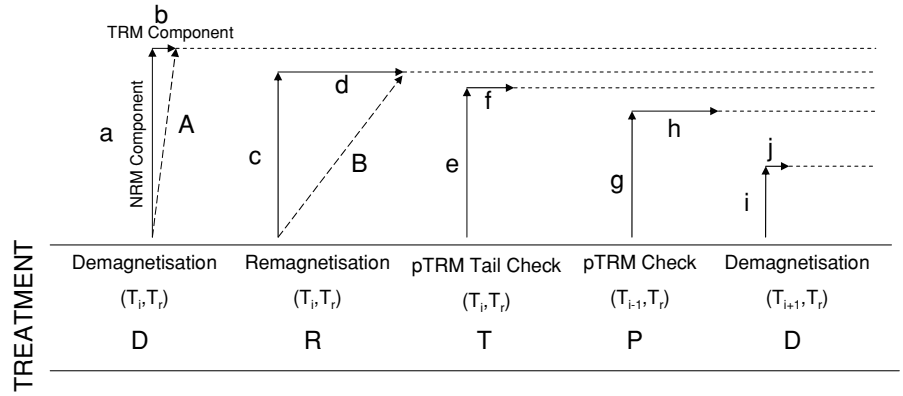


Fig. 2. Schematic diagram showing the measurements (labelled a–j) made after each treatment of the palaeointensity experiments for reference with Table 2 and other figures. Vertical (horizontal) arrows represent the measured NRM (TRM) components. $T_r$ is room temperature.

Table 1. Summary of rock magnetic properties of specimens. See text for details of parameters. The asterisk (*) denotes that this $\chi$(T) curve type was estimated from the shape of the thermal demagnetisation curve.

| Core Sample | $\chi$(T) curve-type | $Q_L$ | VI | $M_{rs}/M_s$ | $H_{cr}/H_c$ |
|---|---|---|---|---|---|
| 008 | L | 2.0 | 7% | | |
| 023 | L | 1.7 | 9% | 0.04 | 2.06 |
| 146 | H | 2.5 | 2% | 0.12 | 2.54 |
| 182 | L | 2.4 | 3% | | |
| 185 | L | 2.0 | 4% | 0.05 | 3.19 |
| 187 | L* | 2.0 | 3% | | |
| 192 | L | 1.9 | 3% | | |
| 279 | C | 2.6 | 4% | 0.12 | 2.49 |
| 283 | H | 2.6 | 1% | 0.12 | 2.51 |
| 287 | L* | 1.5 | 4% | | |
| 289 | L* | 1.4 | 5% | | |

2. The *remagnetisation* treatment (heating and cooling between $T_r$ and $T_i$ in a field of 50 $\mu$T applied along the long axes of the cylindrical specimens).
3. The *pTRM tail check* treatment (identical to 1).
4. The *pTRM check* (for alteration) treatment (heating and cooling between $T_r$ and $T_{i-1}$ in the same field as step 2).

For the purpose of this study, we deconstructed each measurement of remanence that we made during the palaeointensity experiments into components of natural remanent magnetisation (NRM) and laboratory thermoremanent magnetisation (TRM). This was made possible through some special measures adopted by this study. Firstly, we isolated the characteristic component of magnetisation in every sample by subjecting it to an AF demagnetisation treatment (peak field 5 mT was found to be sufficient for this purpose). We then repeated this treatment before *every* measurement that was made through the course of the palaeointensity experiment. Secondly, we chose samples with low inclinations of magnetisation in core coordinates so that the laboratory field, applied along the $z$-axis of the samples during steps 2 and 4 (see above), made an angle of between 45° and 135° with their characteristic components of remanence.

The measurement made after the first AFD treatment and before any thermal treatments was $\mathrm{NRM}_0(X_0, Y_0, Z_0)$. Throughout the rest of the experiment, the NRM component will, ideally, have an identical unit vector. Since the field used in the remagnetisation stages is applied uniquely along the samples' $z$-axes, the $X$ and $Y$ components of the measured vector will therefore reflect only the NRM. The $Z$ component of the NRM can then be calculated from the average of the $X$ and $Y$ components' intensities relative to their original values, i.e.:

$$Z_{nrm}/Z_0 = (X/X_0 + Y/Y_0)/2. \quad (1)$$

The NRM component is then:

$$\mathrm{NRM} = (X^2 + Y^2 + Z_{nrm}^2)^{1/2}. \quad (2)$$

The TRM component is that remaining in the $Z$ measurement:

$$\mathrm{TRM} = |Z - Z_{nrm}| \quad (3)$$

Our process of decomposition of NRM and TRM requires that samples be isotropic with respect to the acquisition of remanence and this appears to be the case for the samples studied here. No magnetic fabric was apparent in measurements of anisotropy of magnetic susceptibility (AMS) made on representative specimens. Furthermore, cleaned palaeomagnetic directions (Biggin *et al.*, 2007a) were close to those expected from the IGRF with no sign of the deflection which would be present if the specimens were anisotropic.

The temperature steps we used in this study ranged from 150°C to 450°C in 50°C steps. PTRM and pTRM tail checks treatments were made at every temperature except 150°C. Values of both the TRM and NRM components were calculated from measurements of the remanence after every treatment in the experiment (Fig. 2). We also made measurements of each sample's room temperature susceptibility after every heating. These measurements together with the cyclic high temperature susceptibility curves and the Arai plots themselves showed that thermochemical alteration was negligible in all samples prior to them being heated to at least 400°C. In order to standardise the results of this study, we use all measurements made in the range $T_r$ to 350°C and omit all those from outside of this range.

The results from a particular sample were only used for the purpose of this study if the values of $X/X_0$ and $Y/Y_0$

Table 2. Palaeointensity results and mean values of pTRM tail parameters (average of different temperature step measurements in bulk of table, average of all samples in bottom row). The $f$, $\beta$, and $q$ parameters are the fraction, standard error/slope, and quality factors (Coe *et al.*, 1978). $PI_{meas}$ and $PI_{exp}$ are, respectively, the measured and expected palaeointensities. Quoted uncertainties are 95% confidence bounds for the mean.

| Specimen | ΔT (°C) | $f$ | $\beta$ | $q$ | $PI_{meas}$ ($\mu$T) | $PI_{exp}$ ($\mu$T) | Tail/ $NRM_0$[1] | TRM/ NRM(Tail)[2] | ΔNRM(Remag)/ $NRM_0$[3] | TRM(Demag)/ $NRM_0$[4] | Tail/ pTRM[5] | TRM(Demag)/ pTRM[6] |
|---|---|---|---|---|---|---|---|---|---|---|---|---|
| 008C | 0–350 | 0.69 | 0.03 | 16.7 | 47.7 | 44.2 | 0.05±0.02 | 1.57±1.11 | −0.05±0.01 | 0.03±0.01 | 13±9% | 8±4% |
| 023C | 0–350 | 0.77 | 0.04 | 15.4 | 38.3 | 44.2 | 0.07±0.02 | 1.77±0.88 | −0.03±0.03 | 0.05±0.03 | 12±14% | 8±2% |
| 146D2 | 0–350 | 0.22 | 0.05 | 3.5 | 80.0 | 44.2 | 0.03±0.01 | 3.25±12.82 | −0.01±0.01 | 0.02±0.01 | 49±23% | 38±51% |
| 182D | 0–350 | 0.78 | 0.03 | 17.7 | 43.2 | 44.1 | 0.05±0.03 | 1.74±1.06 | −0.03±0.02 | 0.03±0.01 | 15±25% | 6±5% |
| 185C2 | 0–350 | 0.69 | 0.04 | 14.1 | 41.2 | 44.1 | 0.05±0.03 | 1.56±0.65 | −0.02±0.01 | 0.02±0.02 | 18±31% | 3±1% |
| 187C | 0–350 | 0.67 | 0.03 | 17.4 | 35.6 | 44.1 | 0.07±0.02 | 2.2±1.14 | −0.02±0.01 | 0.03±0.02 | 24±26% | 6±2% |
| 192C | 0–350 | 0.66 | 0.02 | 34.0 | 40.9 | 44.1 | 0.05±0.01 | 2.05±1.76 | −0.01±0.01 | 0.02±0.01 | 19±22% | 5±2% |
| 279A2 | 0–350 | 0.37 | 0.06 | 4.8 | 43.7 | 43.3 | 0.05±0.02 | 1.94±3.05 | 0.00±0.01 | 0.02±0.01 | 37±20% | 18±11% |
| 283A | 0–350 | 0.18 | 0.07 | 1.9 | 64.0 | 43.3 | 0.02±0.01 | 4.52±1.90 | 0.00±0.01 | 0.01±0.00 | 26±21% | 19±15% |
| 287B | 0–350 | 0.53 | 0.06 | 6.9 | 40.6 | 43.3 | 0.06±0.01 | 2.09±0.42 | −0.02±0.01 | 0.02±0.00 | 25±18% | 9±6% |
| 289B | 0–350 | 0.55 | 0.06 | 6.9 | 41.6 | 43.3 | 0.06±0.01 | 1.78±1.16 | −0.02±0.02 | 0.03±0.01 | 23±18% | 10±5% |
| | | | | | | | 0.05±0.01 | 2.22±0.60 | −0.02±0.01 | 0.03±0.01 | 24±07% | 12±7% |

(1) The mean magnitude of the resultant vectors of components (f - b) and (a - e) in Fig. 2 normalised by the original NRM measurement (2) The mean ratio of components (f - b) to (a - e) as shown in Fig. 2 (3) The mean of (a - c) as shown in Fig. 2 normalised by the original NRM measurement (4) The mean amount of b (or j) as shown in Fig. 2 normalised by the original NRM measurement (5)The value in (1) given as a percentage of the original pTRM ((B - A) in Fig. 2) imparted during the previous remagnetisation treatment (6) The value in (4) given as a percentage of the original pTRM ((B - A) in Fig. 2) imparted during the previous (lower temperature) remagnetisation treatment

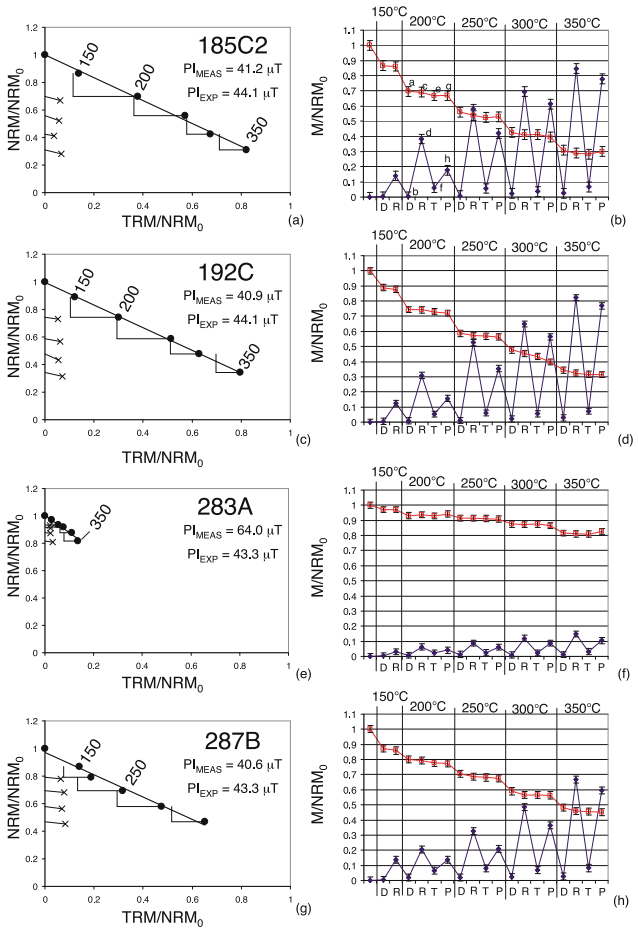


Fig. 3. Arai plots for four samples (left; temperatures are given in degrees Celsius) and associated graphs showing measurements of the isolated NRM (red) and TRM (blue) components (D = Demagnetisation, R = Remagnetisation, T = pTRM Tail check, P = pTRM check). Error bars were calculated using the maximum discrepancy observed in the values of $X/X_0$ and $Y/Y_0$ (Eq. (1)) for that particular sample. The letters refer to the components outlined in Fig. 2 and, although given only for the 200°C step, are applicable to all temperature steps.

were, on average, within 5% of each other. This ensured that noisy or potentially inaccurate data were excluded. A total of 11 samples satisfied these and the earlier criteria and their results will be used in this study.

## 3. Experimental Results

Example Arai plots are given in Fig. 3 and palaeointensity results are presented with their associated quality parameters in Table 2. Over the temperature range $T_r$ to 350°C, the Arai plots of the samples studied here displayed good to excellent linearity (low $\beta$). PTRM checks may fail purely as a result of MD grains being present without any associated alteration (Biggin, 2006). However, in spite of this, 9 of the 11 samples studied here produced DRAT values (Selkin and Tauxe, 2000) of less than 10%. This led to generally high quality results that were, for the most part, reasonably accurate (compare $PI_{meas}$ with $PI_{exp}$, the 'true' palaeointensity taken from the IGRF). Detailed discussion will be given in Biggin *et al.* (2007a) and will not be repeated here.

Table 2 also gives a host of parameters derived from our breakdown of each measurement into NRM and TRM components. These are explained in the footnotes of Table 2 and will be dealt with directly in the text. Since some of the measured values from which the parameters are calculated are extremely small, there is the potential for them to be overwhelmed by experimental errors. Fortunately, the random nature of these errors implies that they will average to zero over a large number of measurements and that we may use statistics to gauge the significance of our measurements. We therefore overcome the problem of experimental noise by averaging the parameters (over multiple temperature steps at the sample level, and over multiple samples) and using the 95% confidence limits for these means (calculated from their standard errors) to ascertain their significance (Table 2).

The pTRM tails detected by the checks are shown as diagonal crosses on the Arai plots in Fig. 3. The positions of these crosses reflects both the tails' TRM and NRM

components and each is joined to the location where it would appear if the samples exhibited perfect SD behaviour.

Such Coe-modified Thellier experiments performed on samples dominated by MD grains are expected to produce Arai plots which are concave-up in shape (Levi, 1977). Since we consider only the low temperature portion of Arai plot, we would expect this curvature to result in palaeointensities which are greater than the expected value. In fact, many of the palaeointensity measurements are small underestimates. This is a result of differences in the rates at which these rocks were cooled in nature and in the laboratory which is dealt with in depth by Biggin *et al.* (2007a). However, even if these effects were not present, the overestimation of the palaeointensity would likely not exceed 20%.

Two exceptions to this general observation were samples 146D2 and 283A (Fig. 3(c)) which produced gross overestimates and which, significantly, had H-type $\chi(T)$ curves and the hardest unblocking temperature spectra of all samples. Just as Biggin (2006) predicted, non-ideal behaviour due to MD grains is exaggerated in these samples because the design of the experiments produces Arai plots with tightly clustered points. For the other samples which are easier to (re)demagnetise, the design of the experiment produces well-spaced Arai plots so that the palaeointensity is not significantly overestimated. This phenomenon is discussed at length in Biggin *et al.* (2007a) and is relevant here only to the extent that we examine the role of pTRM tails in producing it (see Section 4.2).

Also shown in Fig. 3 are graphs showing the evolution of the NRM and laboratory TRM components through the experiments. Their behaviour displays two important differences from that which would be observed in single domain grains. The first of these is that there is some TRM component in every measurement made subsequent to the first remagnetisation treatment. In SD grains, we would expect the TRM component to be non-zero only in measurements made after remagnetisation and pTRM check treatments. What we observe is that 'pTRM tails' affect virtually the entire set of results for every experiment. Many of these individual observations of NRM component, particularly those measured after demagnetisation treatments are within the margin of error for the measurements shown in Fig. 3. However, when averaged over multiple temperatures, they are for the most part significantly different from zero (see the TRM(Demag)/$NRM_0$ column in Table 2). PTRM tails have been shown previously to extend almost to the Curie temperature in MD grains (Bol'shakov and Shcherbakova, 1979) so this observation is not altogether unexpected.

The second aspect of MD behaviour that is apparent here is the continuous removal of NRM through the experiment. Let us be clear: the NRM component should never increase. Where it is observed to do so slightly in these experimental results (e.g. the measurements made after the pTRM check treatments to 150 and 200°C for sample 185C2 shown in Fig. 3(b)), it is most likely a product of experimental noise. In SD grains, the NRM component would be expected to decrease only in the measurements made after simple demagnetisation treatments and remain constant for the three subsequent measurements (i.e. remagnetisation, pTRM tail check, and pTRM check). What we generally observe in our samples is the NRM component decreasing progressively (though not necessarily linearly) during these three treatments.

Although these decreases are small, there is no question of them being artefacts of the experimental noise described above. If this were the case, there would be equal probability of the measured NRM component increasing or decreasing during treatments other than the simple demagnetisation treatment. In fact all 11 of the samples measured exhibit a larger number of decreases than increases and for 7 of these, the difference is significant at the 95% confidence level. With all samples combined, the total number of decreases is 110 whilst the total number of increases is 33. The probability of arriving at this observation by chance is less than 0.00001%.

Each remagnetisation treatment imparts a pTRM which consists of a reciprocal portion and a non-reciprocal portion generally referred to as a tail. It is tempting to imagine the non-reciprocal component behaving as a classical overprint remagnetisation: effectively replacing the NRM component with TRM. Indeed, this is the assumption of most phenomenological models and it offers a qualitative explanation for the decrease in NRM component that we observe in the measurements made after the remagnetisation treatments.

If non-reciprocal components (pTRM tails) do behave as classical overprints then we would expect the amount of TRM component which they comprise to be related to the amount of NRM component that is lost as a result of them being imparted. Specifically, we would expect the ratio between these components to be the same as the ratio between the laboratory field intensity and the true palaeointensity. For example, if the laboratory field was half as strong as the field which originally imparted the NRM, then we would expect the measured pTRM tail to comprise a positive TRM component and a negative NRM component that is twice as large.

The ratio of the laboratory to natural field intensities in this study is approximately 1.1. If cooling rate effects (tending in this study to reduce the effective natural field intensity) are taken into account, this ratio is increased to approximately 1.35 with an absolute maximum value of 1.6 (Biggin *et al.*, 2007a). Table 2 gives the TRM/NRM (Tail) parameter for every sample. This is the mean ratio of TRM gained to NRM lost calculated from the difference between the measurements made after the pTRM tail check and the demagnetisation step. The ratios given in Table 2 should err to lower values than the ratios of field intensities because they assume that no NRM was lost between the remagnetisation and pTRM tail check measurements. It is therefore interesting that, in spite of this, they are generally larger than the expected ratio. With respect to individual samples, this offset in seldom outside of calculated uncertainties. However, when the sample means are combined, the total mean (as shown in the bottom row of Table 2) is distinguishable from the maximum plausible ratio of 1.6 at the 95% confidence level (t-test (Lowry, 1999)). This suggests that, on average, during the process of imparting a non-reciprocal component of pTRM, more TRM component is

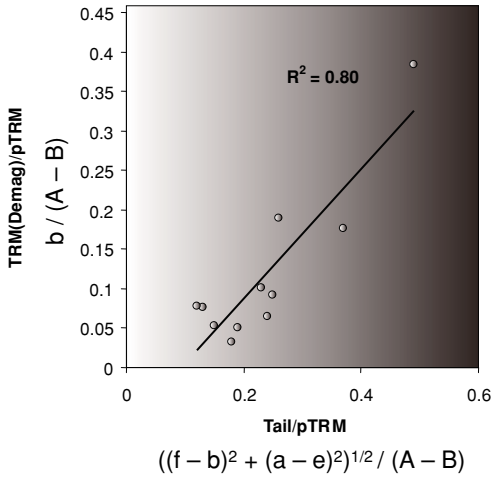


Fig. 4. Average values of normalised TRM (Demag) plotted by sample against average values of normalised measured tail size. Formulae refer to the components labelled in Fig. 2.

added than NRM component is lost. This clash between theory and experiment will be discussed in Section 4.1.

Since part of each non-reciprocal component is visible as a TRM component in the measurements made after the demagnetisation treatments at each temperature step, this opens up the possibility to detect tails (and hence MD behaviour) in palaeointensity experiments such as these without having to make dedicated pTRM tail check treatments. The standard means to detect pTRM tails is to vector subtract the measurement made after the demagnetisation treatment from that made after the pTRM tail check treatment. However, this must then be corrected for intensity and angular differences between the natural and laboratory field (Leonhardt *et al*., 2004) to become a meaningful parameter. In Fig. 4, we compare the mean magnitudes of the results of these calculations with the mean amounts of TRM components detected directly in the measurements made after the demagnetisation treatments (both normalised to the amount of pTRM imparted by the previous remagnetisation stage). There is a strong correlation which supports the idea that pTRM tails can be detected directly in future studies without resorting to dedicated thermal treatments. This issue will be discussed further in Section 4.2.

## 4. Discussion and Conclusions

The experimental results described above have implications for our general understanding of TRM behaviour in MD grains as well as how we undertake palaeointensity experiments in the future. We will now discuss each of these implications in turn.

### 4.1 Implications for our understanding of TRM behaviour in multidomain grains

A number of phenomenological models of MD TRM have been developed in recent years. The pioneer model was that of Fabian (2000, 2001) which faithfully simulated concave-up Arai plots produced by Coe-modified Thellier experiments undertaken with the laboratory field applied parallel to the NRM. This model assumed that the type of pTRM applied in a palaeointensity experiment does not have an associated tail; it is therefore not relevant to the present study.

Yu *et al*. (2004) did include the relevant tails in their simple but effective model. However, their model implicitly allows demagnetisation to occur only during specific demagnetisation treatments in a palaeointensity experiment (and not remagnetisations, pTRM tail checks, etc as observed here). Consequently it is also not relevant to the present study.

Leonhardt *et al*. (2004) and Biggin (2006) modified Fabian's model so that pTRM tails as observed in this study were included. Both of their models predict that the pTRM tails occupy a portion of the blocking temperature spectrum in a manner similar to a conventional pTRM in SD grains. In a palaeointensity experiment then, the action of imparting a pTRM tail is predicted to cause simultaneous demagnetisation and remagnetisation as the TRM component overprints the NRM component. Qualitatively, these models are accurate but they do not predict that the TRM component will be affected to a greater extent than the NRM component as was, on average, observed here. Furthermore, these models do not predict any loss of NRM during pTRM tail check or pTRM check treatments as was frequently observed in these experiments.

In order to explain this observation, we must use the kinematic model derived by Biggin and Poidras (2006) and used to simulate palaeointensity experiments by Biggin (2006). In this model, the behaviour of an assemblage of MD grains undergoing thermomagnetic treatments is governed by the following one-dimensional differential equation:

$$\frac{dm}{dT} = f(T)(uH - vm) \tag{4}$$

where $m$ is the net magnetisation of the assemblage, $H$ is the applied field, $u$ and $v$ are constants, and $f(T)$ is some function of temperature which defines the degree of resistance to changes in the grain's net magnetism. This equation states that the MD system attempts to change its TRM so that its average magnetostatic energy, produced from interaction with the external field and the internal demagnetising field, is minimised but that its ability to make this change is governed by its temperature.

Equation (4) was explicitly solved and used to produce three-dimensional numerical solutions by Biggin (2006). We use the same model here to simulate a Coe-modified Thellier experiment with the field applied perpendicular to the NRM. The Arai plot and the evolution of NRM and TRM components are given in Fig. 5.

This model correctly predicts that the TRM component of the pTRM tail measured by the check at each temperature will, on average, be larger than the NRM component. This model is free to arrive at this result because, unlike the phenomenological models, it is not based on the tenets of blocking and unblocking temperature spectra which, strictly-speaking, are only appropriate for describing TRM in SD grains.

The ratio of the TRM to NRM components in the measurement of the tail is large because the amount of TRM remaining after the pTRM tail check is generally larger than the cumulative amount of NRM lost in both the remagneti-

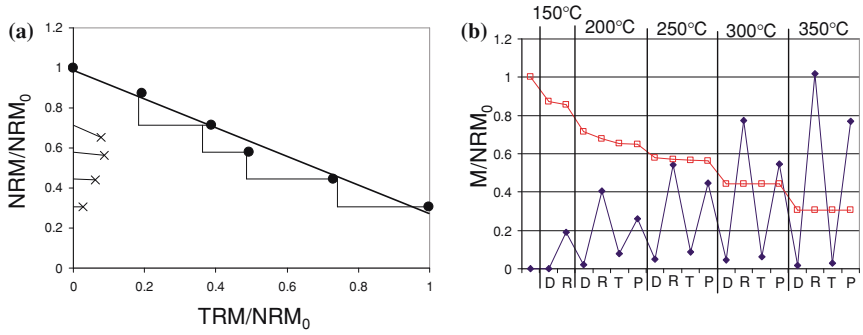


Fig. 5. Arai plot (a) and separated NRM-TRM component graph (b) produced by the kinematic model outlined in Biggin (2006) with SD/MD = 4.

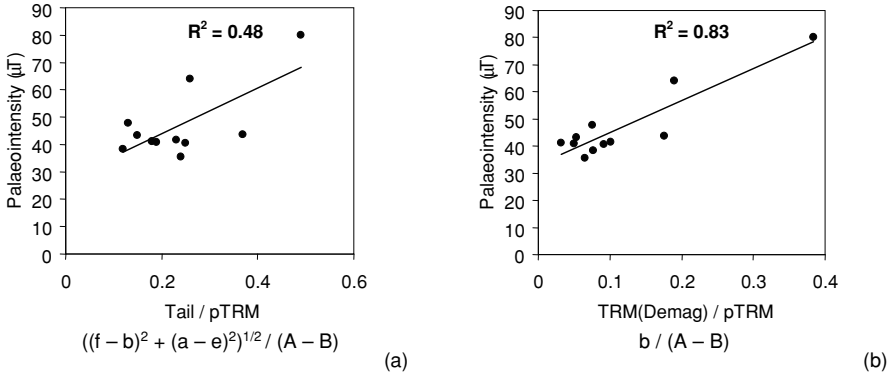


Fig. 6. A comparison of the effectiveness of the conventional tail check method (a) and the new method (b) of detecting overestimation of the palaeointensity due to MD effects. The expected palaeointensity was approximately 43–44.5 $\mu$T but cooling rate effects forced this to be as low as 35 $\mu$T in some cases where MD effects were virtually absent (Biggin *et al.*, 2007a). Formulae refer to the components labelled in Fig. 2.

sation and the pTRM tail check treatments. The reasons for this result are tied to the specific level of disequilibrium—the values of $(uH - vm)$—for the NRM and TRM components during each treatment.

The kinematic model predicts that the ratios should grow larger and larger through the experiment as the NRM component falls and therefore demagnetises less during the remagnetisation and pTRM tail check treatments. This secondary prediction is not strongly supported by the experimental ratios which tend to fluctuate about a constant value. It is not clear whether this inconsistency is a product of the oversimplified theory or the particular experimental conditions (for example, longer hold times being used for higher temperature treatments). The kinematic model also predicts the removal of NRM during pTRM tail check and pTRM check treatments which was observed experimentally.

Overall then, it appears that MD TRM behaviour may be better understood through kinematic non-equilibrium arguments which do not rely on relationships between blocking and unblock temperatures than through extension of Néel's (1955) SD theory to MD grains.

### 4.2 Implications for future palaeointensity studies

The experimental results presented here demonstrate that dedicated pTRM tail check treatments are not necessary in Thellier-type palaeointensity experiments in order to detect pTRM tails. Instead, by following the experimental protocol outlined here, it is possible to detect them directly in the measurements made after the standard demagnetisation treatment. This alone will allow a 25% reduction in the time spent on a standard experiment.

The recently-proposed IZZI technique (Tauxe and Staudigel, 2004) can also detect MD-like behaviour without recourse to specific pTRM tail checks by producing a zigzag-shaped Arai plot. However, the method outlined by the present study (i.e. the measurement of TRM(Demag); see Table 2) has a benefit even over this technique which we will now explain.

Biggin (2006) made a clear prediction that highly intensive Thellier-type experiments which produce points that are closely-spaced on the Arai plot will tend to exaggerate the non-linearity caused by MD grains. This is entirely consistent with the results presented here. The reason for this behaviour is that the pTRM tails can have a greater *cumulative* effect in such intensive experiments. In light of this information, it is apparent that the extent to which non-linear MD behaviour is present in the results of a palaeointensity experiment is itself a function, not only of the total size of the tails (determined by the nature of the sample) but also the extent to which these tails survive following the subsequent higher temperature demagnetisations (determined by the nature of both the sample and the experiment).

Both conventional pTRM tail checks and the IZZI method detect the total amount of pTRM tail produced by a remagnetisation treatment at each temperature. However, the TRM component that is detected directly from the measurements made after each demagnetisation stage (the pa-

rameter TRM(Demag)) is the remnants of the tail that was imparted at the previous lower temperature step. Therefore while tail checks and the IZZI method are sensitive only to the degree of MD behaviour exhibited by a sample, the parameter TRM(Demag) is sensitive to the extent that such MD behaviour will manifest itself in that particular experiment.

Figure 6 demonstrates the usefulness of this. Of the two parameters plotted against one another in Fig. 4, the average normalised tail present after the demagnetisation treatments (TRM(Demag)/pTRM) is shown to be a better predictor of the palaeointensity than the average normalised tail detected using the dedicated checks. This is especially convincing considering that the potential for experimental noise is greater in Fig. 6(b) than 6(a) on account of the smaller signal being measured in the former. If future palaeointensity studies follow the techniques outlined here and measure the mean value of TRM(Demag), then the bias caused by MD grains can be *better* detected than by making explicit pTRM tail check measurements (or, by inference, than using the IZZI method). More data would be required to determine a definitive cutoff but Fig. 6(b) suggests that in general, if the mean value of TRM(Demag)/pTRM does not exceed 10%, then the palaeointensity is unlikely to be excessively overestimated.

The key to this new experimental routine is the pre-measurement demagnetisation treatment at every step which has been attempted previously with mixed results (Coe and Grommé, 1973; McClelland and Briden, 1996; Riisager *et al*., 2004). In this study, an AFD treatment to peak field 5 mT was employed but researchers are obviously free to choose the type and degree of this treatment as they see fit. The mandatory requirements are that the treatment is repeated prior to *every* measurement, that it is sufficient to isolate a convergent component, and that the laboratory field makes an angle between approximately 45 and 135° with this component in order to minimise the potential for error amplification.

Such a pre-measurement demagnetisation has benefits to palaeointensity studies other than allowing the easy detection of pTRM tails. One of these is that, especially when dealing with samples containing MD grains, the Arai plots are far less noisy than those produced by experiments not employing the treatments (Biggin *et al*., 2007b). Additionally, a palaeointensity determination is often significantly affected by the choice of points on the Arai plot to which the straight line is fit. This choice is not always straightforward and therefore a degree of subjectivity affects many palaeointensity measurements. However, in experiments using a pre-measurement demagnetisation, the room-temperature point of the Arai plot should always be the starting point for the straight line. Consequently, a further benefit of employing pre-measurement demagnetisations is that the choice of where to begin the fit of the straight line on the Arai plot becomes automatic and therefore, that the subjectivity associated with the determination is reduced.

A third benefit of using pre-measurement demagnetisations is that, by allowing the decomposition of a measurement into TRM and NRM components (i.e. Eqs. (1)–(3)), they can remove the need for double-heating steps in Thellier-type palaeointensity experiments. The only single-heating method currently practised is the perpendicular method developed by Kono and Ueno (1977). This is a fast and reliable method that, with the exception of microwave experiments, did not prove popular because of the difficulty experienced by many labs in aligning the field perfectly perpendicular to each sample's NRM. The pre-measurement treatment and analytical procedure outlined here can effectively negate this difficulty: the individual NRM and TRM components are separable despite not being exactly orthogonal. This paves the way for a rapid, single-heating *quasi-perpendicular* method that is demonstrated elsewhere (Biggin *et al*., 2007b).

**Acknowledgments.** AJB performed this research while in receipt of a post-doctoral fellowship from the French 'Ministère délégué à la recherche et aux nouvelles technologies'. The authors would like to thank Avto Goguitchaichvili and an anonymous reviewer for helpful comments. This manuscript deals with the methodology associated with absolute palaeointensity determination as well as touching on a fundamental rock magnetic problem. These are just two of the numerous fields that Masaru Kono has made lasting contributions towards during his career and it is with great honour that we continue this work.

## References

Biggin, A. J. and T. Poidras, First-order symmetry of weak-field partial thermoremanence in multi-domain ferromagnetic grains. 1. Experimental evidence and physical implications, *Earth Planet. Sci. Lett*., **245**, 438–453, 2006.

Biggin, A. J. and D. N. Thomas, The application of acceptance criteria to results of Thellier palaeointensity experiments performed on samples with pseudo-single-domain-like characteristics, *Phys. Earth. Planet. Int*., **138**, 279–287, 2003.

Biggin, A. J., First-order symmetry of weak-field partial thermoremanence in multi-domain (MD) ferromagnetic grains: 2. Implications for Thellier-type palaeointensity determination, *Earth Planet. Sci. Lett*., **245**, 454–470, 2006.

Biggin, A. J., M. Perrin, and M. J. Dekkers, A reliable palaeointensity determinations obtained from a non-ideal recorder, *Earth Planet. Sci. Lett*., **247**, 545–563, 2007a.

Biggin, A. J., M. Perrin, and J. Shaw, A comparison of a Quasi-Perpendicular method of absolute palaeointensity determination with other thermal and microwave techniques, *Earth Planet. Sci. Lett*., **247**, 564–581, 2007b.

Bol'shakov, A. S. and V. V. Shcherbakova, A thermomagnetic criterion for determining the domain structure of ferrimagnetics, *Izv. Acad. Sci. USSR Phys. Solid Earth*, **15**, 111–117, 1979.

Coe, R. S., Palaeointensities of the Earth's magnetic field determined from Tertiary and Quaternary rocks, *J. Geophys. Res*., **72**, 3247–3262, 1967.

Coe, R. S. and C. S. Grommé, A comparison of three methods of determining geomagnetic paleointensities, *J Geomag. Geoelectr.*, **25**, 415–435, 1973.

Coe, R. S., C. S. Grommé, E. A. Mankinen, Geomagnetic paleointensities from radiocarbon dated lava flows on Hawaii and the question of the Pacific non-dipole low, *J. Geophys. Res.-Solid Earth*, **83**, 1740–1756, 1978.

Dunlop, D. J. and Ö. Özdemir, Beyond Neel's theories: thermal demagnetization of narrow-band partial thermoremanent magnetizations, *Phys. Earth. Planet. Int*., **126**, 43–57, 2001.

Fabian, K., Acquisition of thermoremanent magnetization in weak magnetic fields, *Geophys. J. Int*., **142**, 478–486, 2000.

Fabian, K., A theoretical treatment of paleointensity determination experiments on rocks containing pseudo-single or multi domain magnetic particles, *Earth Planet. Sci. Lett*., **188**, 45–58, 2001.

Goguitchaichvili, A., J. Morales, J. Urrutia-Fucugauchi, and A. M. Soler, On the use of continuous thermomagnetic curves in paleomagnetism: a cautionary note, *Cr Acad Sci Ii A*, **333**, 699–704, 2001.

Kono, M. and N. Ueno, Palaeointensity determination by a modified Thellier method, *Phys. Earth. Planet. Int*., **13**, 305–314, 1977.

Leonhardt, R., D. Krasa, and R. S. Coe, Multidomain behavior during Thellier paleointensity experiments: a phenomenological model, *Phys. Earth. Planet. Int.*, **147**, 127–140, 2004.

Levi, S., The effect of magnetite particle size on palaeointensity determinations of the geomagnetic field., *Phys. Earth. Planet. Int.*, **13**, 245–259, 1977.

Lowry, R., Concepts and Applications of Inferential Statistics, 1999.

McClelland, E. and J. C. Briden, An improved methodology for Thellier-type paleointensity determination in igneous rocks and its usefulness for verifying primary thermoremanence, *J. Geophys. Res.*, **101**, 21995–22013, 1996.

Néel, L., Some theoretical aspects of rock magnetism, *Adv. Phys.*, **4**, 191–242, 1955.

Perrin, M., Paleointesity determination, domain structure, and selection criteria, *J. Geophys. Res.*, **103**, 30591–30600, 1988.

Prévot, M., A. Lecaille, and E. A. Mankinen, Magnetic effects of maghematization of oceanic crust, *J. Geophys. Res.*, **86**, 4009–4020, 1981.

Riisager, P. and J. Riisager, Detecting multidomain magnetic grains in Thellier palaeointensity experiments, *Phys. Earth. Planet. Int.*, **125**, 111–117, 2001.

Riisager, J., P. Riisager, X. X. Zhao, R. S. Coe, and A. K. Pedersen, Paleointensity during a chron C26r excursion recorded in west Greenland lava flows, *J. Geophys. Res.*, **109**, B04107 1–12, 2004.

Selkin, P. A. and L. Tauxe, Long-term variations in palaeointensity, *Philos. T. Roy. Soc. A*, **358**, 1065–1088, 2000.

Shashkanov, V. A. and V. V. Metallova, Violation of Thellier's law for partial thermoremanent magnetisation, *Izv. Earth Phys.*, **8**, 180–184, 1972.

Shcherbakov, V. P., V. V. Shcherbakova, and Y. K. Vinogradov, On a thermomagnetic criterion for the identification of the domain structure, *Izv. Phys. Solid Earth*, **37**, 244–248, 2001a.

Shcherbakov, V. P., V. V. Shcherbakova, Y. K. Vinogradov, and F. Heider, Thermal stability of pTRMs created from different magnetic states, *Phys. Earth. Planet. Int.*, **126**, 59–73, 2001b.

Tauxe, L. and H. Staudigel, Strength of the geomagnetic field in the Cretaceous Normal Superchron: New data from submarine basaltic glass of the Troodos Ophiolite, *Geochem. Geophys. Geosys.*, **5**, Art. No. Q02H06, 2004.

Thellier, E., Sur l'aimantation des terres cuites et ses applications géophysique, *Ann. Inst. Phys. Globe Univ. Paris*, **16**, 157–302, 1938.

Thellier, E. and O. Thellier, Sur l'intensité du champ magnétique terrestre dans la passé historique et géologique, *Ann. Géophys.*, **15**, 285–376, 1959.

Yu, Y. J. and D. J. Dunlop, On partial thermoremanent magnetization tail checks in Thellier paleointensity determination, *J. Geophys. Res.*, **108**, Art. No. 2523, 2003.

Yu, Y. J., L. Tauxe, and A. Genevey, Toward an optimal geomagnetic field intensity determination technique, *Geochem. Geophys. Geosys.*, **5**, doi:10.1029/2003GC000630, 2004.

A. J. Biggin (e-mail: biggin@geo.uu.nl) and M. Perrin